ELSEVIER

Catalysis Today 49 (1999) 441–451

CATALYSIS TODAY

Recent progress in diffuse reflectance spectroscopy of supported metal oxide catalysts

Bert M. Weckhuysen*, Robert A. Schoonheydt

Centrum voor Oppervlaktechemie en Katalyse, Departement Interfasechemie, K.U. Leuven, Kardinaal Mercierlaan 92, 3001 Heverlee, Belgium

Abstract

Diffuse reflectance spectroscopy is a suitable technique for studying heterogeneous catalysts, as both d–d and charge transfer transitions of supported transition metal ions can be probed. Within the past several years, new developments have resulted in a more detailed understanding of the surface chemistry of supported metal oxide catalysts. In this review, the fundamental advances of the use of diffuse reflectance spectroscopy in the field of heterogeneous catalysis will be discussed. It will be shown that (1) oxidation states can be spectroscopically quantified in well-defined conditions; (2) chemometrical techniques are crucial for an unbiased analysis of the spectra; (3) in situ spectroscopy, in combination with experimental design and on line catalytic measurements, allows the development of relevant structure–activity relationships, and (4) the reduction kinetics of supported metal oxides can be evaluated.

Keywords: Diffuse reflectance spectroscopy; Chemometrics; Quantitation; SIMPLISMA

1. Introduction

Identifying and quantifying oxidation states and coordination environments of transition metal ions (TMIs) in supported metal oxide catalysts is crucial for understanding their chemistry and catalytic action. Various spectroscopic techniques, such as X-ray photoelectron spectroscopy (XPS), electron spin resonance (ESR) and Raman spectroscopy (RS), are available to perform this task, but the heterogeneous nature of supported metal oxide catalysts, and the simultaneous occurrence of several oxidation states of TMIs makes the analysis difficult, and in most cases, only qualitative information is obtained.

Diffuse reflectance (DRS) spectroscopy in the ultraviolet, visible and near-infrared region is, in principle, the most versatile spectroscopic technique, as both d–d and charge transfer (CT) transitions can be probed [1,2]. One of the advantages of DRS spectroscopy is that the obtained information is directly chemical since the outer shell electrons are probed. Furthermore, the DRS technique can be used under in situ conditions, and is quantitative in nature. The main disadvantage is that diffuse reflectance spectra are complex, and usually encompasses several broad and overlapping bands. To avoid biased spectral analysis, chemometrical techniques need to be employed.

In this review, the fundamental advances of the use of DRS spectroscopy in the field of heterogeneous catalysis will be discussed. No attempt has been made to compile an exhaustive list of references to all the

*Corresponding author. Fax: +32-16-32-19-98; e-mail: bert.weckhuysen@agr.kuleuven.ac.be

0920-5861/99/$ – see front matter
PII: S0920-5861(98)00458-1

work that has been published since the last review article on DRS spectroscopy which appeared in the mid 1980s [2]. Rather, we have selected what, we feel, are the most important developments over the past several years. In Sections 1 and 2, the theory and practice of the DRS technique will be briefly summarized. Sections 3–6 will focus on new developments in the field; i.e., quantitative DRS spectroscopy, the application of chemometrics for an unbiased spectral analysis and the use of in situ measurements to develop structure–activity relationships and to evaluate the reduction kinetics of supported metal oxides. Supported chromium oxide catalysts were selected as an example because they are extensively studied in our laboratory. The review paper closes with some concluding remarks and an outlook into the future.

2. Theory

DRS spectroscopy is a spectroscopic technique based on the reflection of light in the ultraviolet (UV), visible (VIS) and near-infrared (NIR) region by a powdered sample. Kortüm [1] has discussed the theoretical and practical principles of diffuse reflectance in great detail in his book. As a consequence, it is sufficient to give a concise background of the DRS technique. For detailed explanations and discussions-in-depth, we refer to several excellent review papers [2–5].

In a DRS spectrum the ratio of the light scattered from an infinitely thick layer and the scattered light from an ideal non-absorbing reference sample is measured as a function of the wavelength λ. The illumination of powdered samples by incident radiation leads to diffuse illumination of the samples. The incident light is partially absorbed, partially scattered. The scattered radiation, emanating from the sample is collected in an integration sphere and detected. This is schematically illustrated in Fig. 1. The basic equation for the phenomenological description of diffuse reflection is the radiation transfer equation:

$$\frac{-\mathrm{d}I}{\kappa\rho\,\mathrm{d}S} = I - \frac{j}{\kappa}, \tag{1}$$

where I is the incident light intensity of a given wavelength; $\mathrm{d}I/\mathrm{d}S$ the change of the intensity with the pathlength $\mathrm{d}S$; ρ the density of the medium; κ an attenuation coefficient corresponding with the total radiation loss due to absorption and scattering; j is the scattering function.

Eq. (1) can be solved by introducing simplifications which are related with easily attainable experimental conditions. These ideas, first suggested by Schuster and later on further developed by Kubelka and Munk, simplify the solution of the radiative transfer Eq. (1), known as the Schuster–Kubelka–Munk (S–K–M) theory.

In this theory, the incident and scattered light flux are approximated by two fluxes I and J perpendicular to the surface of the powdered sample, but in the opposite direction. This is illustrated in Fig. 2. I is the flux of monochromatic diffuse illumination, whereas J is the flux of diffusively scattered light. If the sample is infinitely thick, the diffuse reflection of the sample (R_∞) is related to an apparent absorption (K) and apparent scattering coefficient (S) via the Schuster–Kubelka–Munk (S–K–M) or Kubelka–Munk (K–M) function:

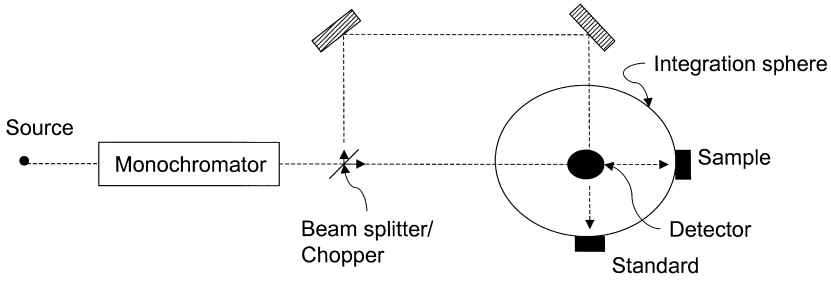

Fig. 1. Schematic overview of a diffuse reflectance spectrophotometer with integration sphere.

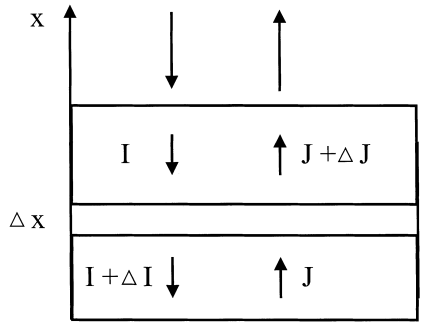

Fig. 2. The Schuster–Kubelka–Munk approximation in diffuse reflectance spectroscopy. The incident and remitted light fluxes are approximated by two opposite fluxes, perpendicular to the surface of the infinitely thick sample layer (Marcel Dekker, Copyright 1984).

$$F(R_\infty) = \frac{(1-R_\infty)^2}{2R_\infty} = \frac{K}{S}. \quad (2)$$

Eq. (2) is valid under the following conditions:

1. diffuse monochromatic irradiation of the powdered sample;
2. isotropic light scattering;
3. an infinite layer thickness;
4. a low concentration of TMIs;
5. a uniform distribution of TMIs;
6. absence of fluorescence.

K and S are characteristic of the material under investigation, and the true absorption coefficient σ_ν and true scattering coefficient σ_ν at frequency ν are related to K and S via

$$\alpha_\nu = \eta K \text{ and } \sigma_\nu = \chi S. \quad (3)$$

Values of η and χ are plotted and tabulated for a range of K/S values, and it is shown that in the limit of small absorptions η and χ are equal to 1/2 and 4/3, respectively.

It follows from Eqs. (2) and (3) that

$$\frac{\alpha_\nu}{\alpha_\nu} = \frac{(1-R_\infty)^2}{2R_\infty}\frac{\eta}{\chi}. \quad (4)$$

Eqs. (3) and (4) are introduced by Klier [6], and the ratio η/χ is fairly constant and equal to 3/8 for values of K/S between 0 and 0.3. For strongly absorbing catalysts (K/S>0.3 or R_∞<0.5) η/χ decreases. Thus, at low concentrations of supported TMIs, Eq. (2) is a good representation of the absorbing spectrum, and allows a quantitative determination of the TMI according to:

$$F(R_\infty) = \frac{(1-R_\infty)^2}{2R_\infty} = \frac{K}{S} = \frac{\alpha C_{\mathrm{TMI}}}{S} = kC_{\mathrm{TMI}}. \quad (5)$$

When at a given wavelength λ, S is constant, Eq. (5) gives a linear relation between $F(R_\infty)$ and the TMI-concentration, C_{TMI}. The coefficients α and k are proportionality constants.

DRS is a particularly suitable technique for studying the speciation of supported TMIs because it measures both their d–d transitions and charge transfer bands. This is illustrated in Table 1 for some reference chromium compounds [7]. It is clear that the number, wavelength and intensity of the d–d bands depend on the oxidation state (Cr^{2+} vs Cr^{3+}) and coordination environment (octahedral, tetrahedral, etc.), whereas the CT transitions of the type $O \rightarrow Cr^{6+}$ (d^0) are

Table 1
Band maxima of the DRS spectra of some reference Cr-compounds

Compound	Coordination geometry and oxidation state	Absorption bands (nm)[a]	Color
K_2CrO_4 (solution)	T_d, Cr^{6+}	440 (sh, vw), 370 (s), 275 (s)	Yellow
K_2CrO_4 (solid)	T_d, Cr^{6+}	459 (s), 340 (s), 265 (s), 229 (s)	Yellow
$K_2Cr_2O_7$ (solution)	T_d, Cr^{6+}	440 (w), 352 (s), 255 (s)	Orange
$K_2Cr_2O_7$ (solid)	T_d, Cr^{6+}	526 (s, br), 332 (s), 262 (s), 229 (s)	Orange–red
$Cr(NO_3)_3{\cdot}9H_2O$ (solution)	O_h, Cr^{3+}	575 (s), 410 (s), 303 (s)	Green
$Cr(NO_3)_3{\cdot}9H_2O$ (solid)	Dist O_h, Cr^{3+}	575 (s), 410 (s), 304 (s), 263 (sh)	Green
$Cr(H_2O)_6^{2+}$ (solution)	O_h, Cr^{2+}	769 (s)	Blue
K_2CrCl_4 (solid)	Distorted T_d, Cr^{2+}	1430 (s)	Blue
Cr_2O_3 (solid)	Distorted O_h, Cr^{3+}	714 (sh), 645 (sh), 595 (s), 461 (s), 351 (s), 274 (s)	Green

[a]s: strong; m: medium; w: weak; vw: very weak; sh: shoulder; br: broad.

responsible for the intense yellow–orange color of calcined chromium oxide catalysts.

3. Practical considerations

As mentioned above, the S–K–M equation is only valid under well-defined conditions [2]. Conditions (a), (b) and (d) are most closely met when the medium consists of densely packed, randomly shaped particles whose sizes are comparable with or smaller than the wavelength of the light. The infinite thickness criterion (condition (c)) is usually reached for catalyst layers of 5 mm thickness, although supported metal oxide catalysts made from some silicas (e.g., Cab-O-Sil Cabot and Aerosil Degussa) may need thicker layers. For work in vacuum, adsorption studies or catalytic experiments specially designed cells are necessary with silica windows with extremely low OH and H_2O contents. It is also advisable to sieve the catalyst and to work with fractions of the same size range.

All spectrometers of the major companies have commercially available diffuse reflectance attachments, with fully automated acquisition, background subtraction and file storage. The latter allows the user to calculate the S–K–M function according to Eq. (2), and to perform band decomposition routines and chemometrical analysis.

The choice of reference materials is also crucial for reliable DRS measurements. Excellent reference materials are totally reflecting over an as wide as possible frequency range. In addition, they must be stable towards water and other chemical compounds. Indeed, the presence of contaminants may result in a decrease of the reflection in the NIR (e.g., water), VIS (e.g., chlorophyll) and UV (e.g., aromatics) region. Nowadays, polytetrafluoroethylene (PTFE) is preferred over the more traditional reference materials (MgO and $BaSO_4$) because of its superior NIR performances. It is also important to notice that reference materials suffer from aging, and that they must be regularly checked, and, if necessary, replaced. An alternative way of working is to use the bare oxide support (e.g., SiO_2, Al_2O_3, ZrO_2 and TiO_2) as a reference material. In this way, one can correct for the light absorption by the support which may hamper the investigation of the supported TMI. This is especially important for TMIs with CT transitions in the UV region (e.g., Re^{7+}). Furthermore, when reference material and supported metal oxide catalysts are in the same type of DRS cells, effects due to these DRS cells are eliminated.

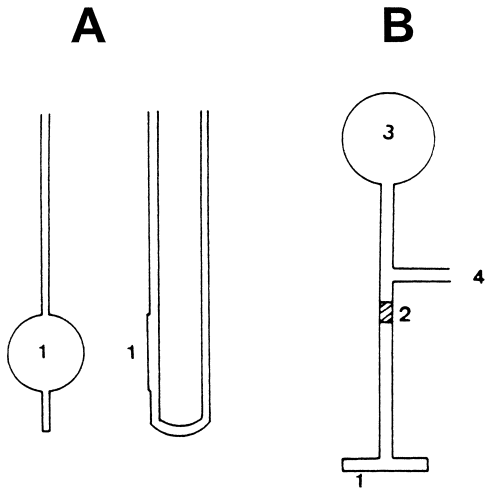

Fig. 3. DRS cells: (1) suprasil; (2) quartz-Pyrex transitions; (3) pretreatment volumes; (4) exit to vacuum line (Marcel Dekker, Copyright 1984).

Fig. 3 illustrates two types of quartz cells currently in use in our laboratory for measurements of supported metal oxide catalysts in the dehydrated state, after adsorption of probe molecules, etc. Type A allows pretreatment of the samples with the desired gas flow through the catalyst bed, whereas Type B is designed for measurements in vacuum or static atmospheres. Fig. 4(A) shows a specially designed Praying Mantis diffuse reflection attachment (Harrick) for in situ measurements. Its construction with two ellipsoidal mirrors provides that mainly the diffuse component of the reflected light is captured [8]. In conjunction with this attachment, a stainless steel reaction chamber (Fig. 4(B)) can be used with quartz windows and with three gas ports for evacuating the chamber and/or for introducing gas. The chamber can be used under static or dynamic conditions, and in the latter case, the gases can be on line analyzed by gas chromatography.

4. Quantitative spectroscopy

In this section, the application of Eq. (5) to quantify different oxidation states of supported metal oxides

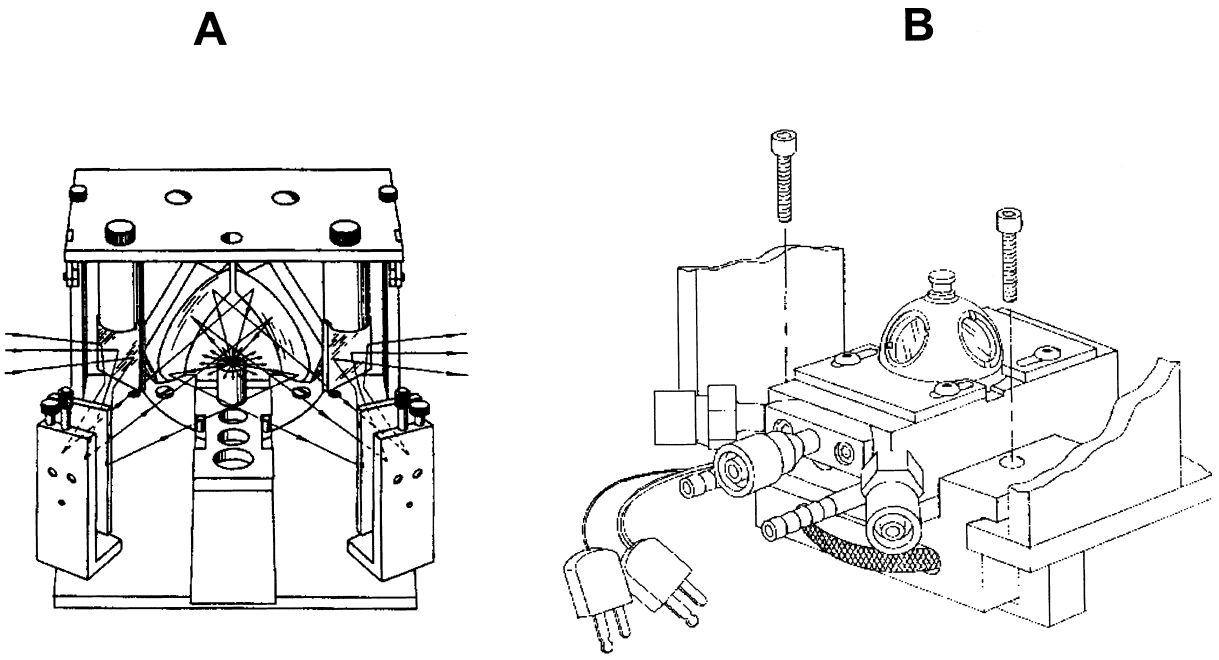

Fig. 4. In situ DRS cell: (A) praying mantis diffuse reflection attachment and (B) stainless steel reaction chamber.

will be illustrated by taking Cr-based catalysts as an example [7,9,10]. An overview of the method is given in Fig. 5 [7]. In the first step, the total Cr content is determined by chemical analysis, whereas the amount of Cr^{5+} is spectroscopically quantified by double integration of the ESR spectra. In the second step, DRS is used to quantify the amount of Cr^{6+} and Cr^{3+} by using appropriate calibration lines. Finally, the amount of Cr^{2+} is obtained by difference.

The method of quantitative DRS is as follows [7,8]. In the first step, series of DRS spectra differing in one parameter (Cr loading, reduction temperature, support composition, etc.) are measured by using an experimental set-up, illustrated in Fig. 1. An example of such set of DRS spectra is given in Fig. 6 for 0.1 wt% Cr/Al_2O_3 catalysts treated in CO for 30 min at different temperatures. The DRS spectra show the presence of two intense CT transitions

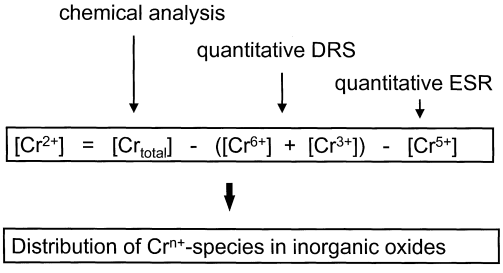

Fig. 5. Quantitative method for quantitation of different Cr oxidation states on amorphous supports (American Chemical Society, Copyright 1996).

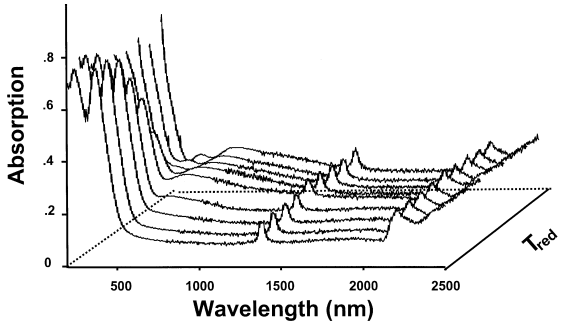

Fig. 6. DRS spectra of 0.1 wt% Cr/Al_2O_3 catalysts as a function of reduction temperature (American Chemical Society, Copyright 1996).

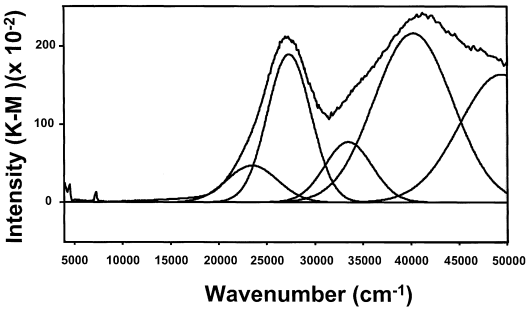

Fig. 7. Deconvoluted DRS spectrum of a calcined 0.1 wt% Cr/Al_2O_3 catalyst (American Chemical Society, Copyright 1996).

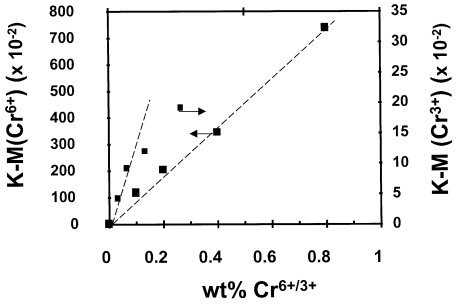

Fig. 8. DRS calibration lines of Cr^{6+} and Cr^{3+} (American Chemical Society, Copyright 1996).

around 370 nm (27 000 cm^{-1}) and 250 nm (40 000 cm^{-1}), which are typical of Cr^{6+} (Table 1). These CT transitions decrease in intensity with increasing reduction temperature. At the same time, new bands appear in the VIS region, which increase in intensity with increasing reduction temperature. These bands are typical for the presence of reduced $Cr^{3+/2+}$ (Table 1).

In the second step, each spectrum is decomposed in a consistent set of Gaussian bands due to Cr^{6+}, pseudo-octahedral Cr^{3+} and pseudo-octahedral Cr^{2+} with a commercial software package entitled Grams/386 (Galactic Industries). An example of such operation is illustrated in Fig. 7 for a calcined Cr/Al_2O_3 catalyst, which shows the four allowed transitions of a supported chromate species, and one Gaussian curve above 222 nm (45 000 cm^{-1}) for the support. An appropriate Cr^{6+}-calibration line can then be obtained by plotting the K–M intensity of the 370 nm (27 000 cm^{-1}) band of chromate as a function of the Cr loading. This is illustrated in Fig. 8, and the obtained calibration line is almost linear. This is clearly not the case for the Cr^{3+}-calibration line, which deviates from linearity above 0.1 wt% Cr^{3+}. Quantitation gives the concentration of Cr^{6+}, Cr^{5+}, Cr^{3+} and Cr^{2+} after different pretreatments. This is shown in Fig. 9. After calcination, Cr^{6+} is the dominant species and only traces of Cr^{5+} are present, which are not observable in the DRS spectra. After reduction, Cr^{6+} is converted to mainly Cr^{3+} and some Cr^{5+} and Cr^{2+}. Upon recalcination, Cr^{3+} is partially reoxidized to Cr^{6+} and a considerable amount is stabilized under Cr_2O_3 form or dissolved in the alumina support. The latter can be envisaged as Cr^{3+}-ions, which occupy the

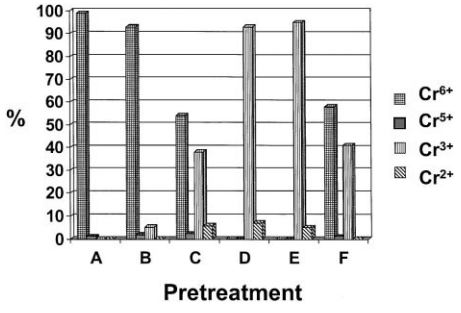

Fig. 9. Distribution of Cr^{6+}, Cr^{5+}, Cr^{3+} and Cr^{2+} on alumina as a function of pretreatment: (A) calcination at 550°C; (B) reduction at 200°C; (C) reduction at 300°C; (D) reduction at 400°C; (E) reduction at 600°C and (F) recalcination at 550°C (American Chemical Society, Copyright 1996).

empty – octahedrally coordinated – vacancies in the γ-Al_2O_3.

This method is also applicable to Cr/SiO_2 and Cr/SiO_2·Al_2O_3 catalysts, at least for low Cr loadings [7]. Comparison between different amorphous supports indicates that the Cr^{2+}:Cr^{3+} ratio increases with increasing SiO_2 content of the support. Thus, SiO_2-rich supports prefer Cr^{2+}-ions, while on alumina mainly Cr^{3+} is present. All these spectroscopic observations are in line with temperature programmed reduction measurements on the same set of Cr-based catalysts [10]. Thus, an average oxidation state of 2 and 3 was obtained after reduction with CO for Cr/SiO_2 and Cr/Al_2O_3 catalysts, whereas Cr/SiO_2·Al_2O_3 catalysts have an intermediate average oxidation state.

In summary, the DRS technique allows the quantitative determination of Cr^{6+}, Cr^{3+} and Cr^{2+} on amorphous supports, at least for low Cr loadings. The

method is based on a detailed analysis of the DRS spectra, which were measured under well-defined conditions as a function of one parameter. It is also important to notice that there is a need for good reference spectra of specific coordination geometries of supported TMIs. Indeed, the obtained information on coordination geometries is rather vague; e.g., the presence of 'pseudo-octahedrally' coordinated Cr^{3+}, and the commercially available TMI compounds are not (always) good reference models. Hopefully, theoretical calculations on models of TMIs will lead in the future to a more detailed description of the coordination geometries.

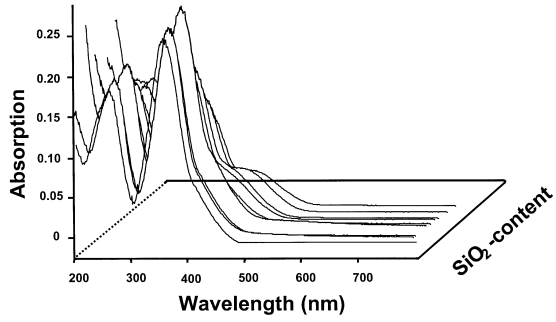

Fig. 10. DRS spectra of 0.2 wt% $Cr/SiO_2{\cdot}Al_2O_3$ catalysts as a function of the SiO_2:Al_2O_3 ratio (Academic Press, Copyright 1997): the front curve with no shoulder at 450 nm is that for a pure Al_2O_3 support, whereas the curve with the most pronounced shoulder at 450 nm is that for a pure SiO_2 support.

5. Chemometrics

Fig. 6 clearly illustrates the difficulties mostly encountered in the analysis of DRS spectra of supported metal oxide catalysts; i.e., experimental DRS spectra are a combination of spectra of individual oxidation states and/or coordination environments of a TMI, in this case tetrahedral Cr^{6+}, pseudo-octahedral Cr^{3+} and pseudo-octahedral Cr^{2+}. This makes spectral analysis difficult, and unbiased information can only be obtained by applying chemometrical techniques, such as principal component analysis (PCA), factor analysis (FA) and partial least squares (PLS). Details about these techniques can be found in several textbooks and research papers [11–14]. The general scheme is as follows: the data matrix *D*, consisting of *n* spectra, each with *m* datapoints, is decomposed as a linear combination of spectra of independent pure components, each with a specific weight. These weights are proportional to the concentrations of the pure components in the mixtures in accordance with the equivalent of Beer's law, namely the Kubelka–Munk function (Eq. (2)).

An interesting chemometrical technique for spectral analysis is SIMPLISMA (simple-to-use-interactive-self-modeling-analysis) developed by Windig [15–17], because it gives not only the number of pure components and their spectra, but the researcher can also intervene and decide by himself whether to accept a pure component or not. An example of the application of the SIMPLISMA technique is given in Fig. 10 for DRS spectra of hydrated $Cr/SiO_2{\cdot}Al_2O_3$ catalysts as a function of the $SiO_2{\cdot}Al_2O_3$ ratio [18]. Four pure spectra are revealed in the DRS spectra of supported Cr catalysts, which are shown in Fig. 11: Component A with three characteristic bands at 493 nm (20 300 cm^{-1}), 327 nm (30 600 cm^{-1}) and 227 nm (44 100 cm^{-1}); component B with three bands at 402 nm (24 900 cm^{-1}), 273 nm (36 600 cm^{-1}) and 220 nm (45 500 cm^{-1}); component C appeared at 565 nm (17 700 cm^{-1}); and component D absorbs in the region 350–270–204 nm (28 600–37 000–49 000 cm^{-1}). Components A and B are due to chromate and dichromate, respectively (Table 1), and their relative ratio increases with decreasing SiO_2:Al_2O_3 ratio. Component C is assigned to pseudo-octahedral Cr^{3+} (Table 1), while component D is a support band. The same analysis can be successfully applied on calcined and reduced supported Cr catalysts [18]. Thus, the SIMPLISMA technique is a viable alternative to the earlier developed Grams/386 method, and

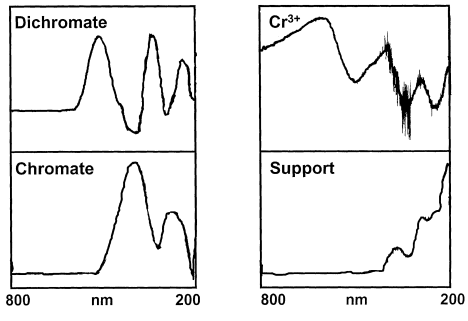

Fig. 11. Pure component spectra of the DRS spectra of Fig. 10 (Academic Press, Copyright 1997).

we propose this method as an interesting tool for investigating complex spectra of supported metal oxide catalysts.

6. In situ spectroscopy

The in situ DRS cell of Fig. 4, in combination with on line gas chromatography (GC) analysis, can be used for the development of quantitative structure–activity relationships in the field of heterogeneous catalysis. This will be illustrated for the dehydrogenation of isobutane over supported chromium oxide catalysts.

This recently developed method involves a four-pronged approach [19,20]. In the first step, the number of required experiments was optimized by using an experimental design. Five factors were selected to describe the dehydrogenation process; i.e., SiO_2:Al_2O_3 ratio of the support, expressed as the isoelectric point (IEP) (X_1), Cr loading (X_2), gas composition (X_3), reaction temperature (X_4) and reaction time (X_5), and a five-level circumscribed central composite experimental design, generated by MODDE for Windows (Umetri AB), resulted in a set of 30 experiments.

Secondly, the dehydrogenation activity was measured by on line GC analysis, respectively. This operation allowed to develop a quantitative relationship between the different factors and the dehydrogenation activity, expressed as $y^{1/2}$:

$$y^{1/2}(\%) = 2.284 - 0.195 \cdot X_1 + 0.121 \cdot X_2 - 0.132 \cdot X_3 - 9.540 \times 10^{-4} \cdot X_4 - 0.0610 \cdot X_5 + 4.941 \times 10^{-3} \cdot X_3^2 + 5.875 \times 10^{-4} \cdot X_5^2 + 5.137 \times 10^{-4} \cdot X_1 \cdot X_4 - 4.480 \times 10^{-3} \cdot X_2 \cdot X_3 + 8.008 \times 10^{-4} \cdot X_3 \cdot X_5. \quad (6)$$

Eq. (6) allows to calculate the conditions for maximum dehydrogenation activity over supported chromium oxide catalysts. The following conditions were obtained: X_1=8; X_2=7.5; X_3=2; X_4=500 and X_5=10. Thus, a maximum conversion is obtained after 10 min for a 7.5 wt% Cr/Al_2O_3 catalyst at 500°C with a mixture of 2% isobutane in N_2. In order to visualize Eq. (6), one can make conversion plots, as illustrated in Fig. 12. This figure predicts the catalytic activity after 10 min for a supported chromium oxide catalyst

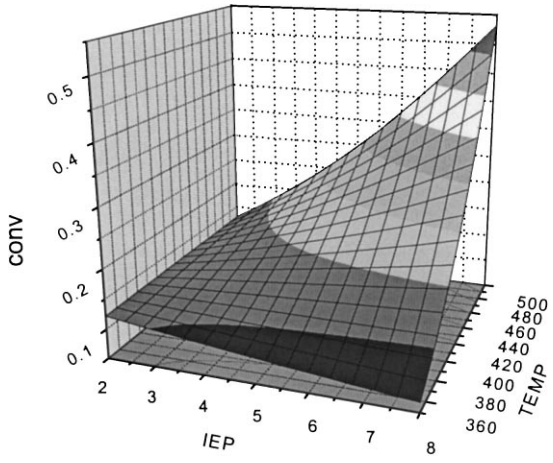

Fig. 12. Conversion surface plot of the isoelectric point of the support and the Cr loading (the reaction temperature, gas composition and reaction time are 500°C, 2% isobutane and 10 min, respectively).

at 500°C in a mixture of 2% isobutane in N_2 as a function of the support composition and the Cr loading. It is clear that the dehydrogenation activity gradually increases with increasing IEP of the support and with increasing Cr loading.

Thirdly, the Cr-speciation was measured by in situ UV–Vis DRS spectroscopy. An example of a set of in situ DRS spectra is given in Fig. 13. This is an experiment with a 0.5 wt% Cr/SiO_2 catalyst treated at 350°C in 2% isobutane. Fig. 13 shows a gradual decrease of absorption maxima around 360 (27 700 cm^{-1}) and 450 nm (22 200 cm^{-1}) with increasing reaction time at the expense of a new weak

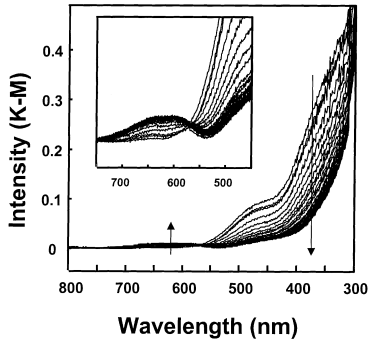

Fig. 13. In situ DRS spectra of 0.5 wt% Cr/SiO_2 catalyst treated at 350°C in 2% isobutane in N_2 as a function of time.

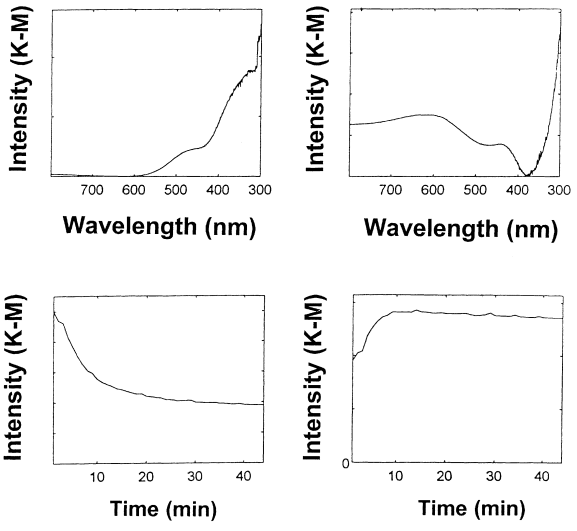

Fig. 14. Pure component spectra of the in situ DRS spectra of Fig. 12.

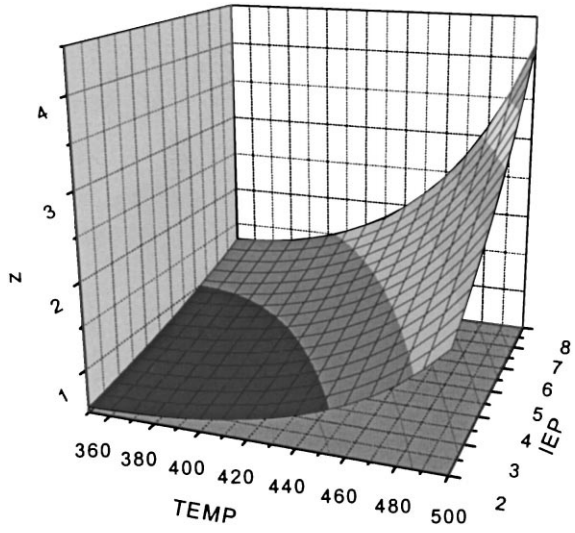

Fig. 15. Reduced chromium surface plot of the reaction temperature and the isoelectric point of the support (the chromium loading is 7.5 wt%).

band with an absorption maximum at around 625 nm (16 000 cm^{-1}). The insert of Fig. 13 illustrates the presence of an isobestic point, suggesting the presence of two different Cr-species. By applying the SIMPLISMA technique to the set of DRS spectra of Fig. 14, two pure component spectra were obtained. The two pure component spectra have absorption maxima around 360 (27 700 cm^{-1}) and 625 nm (16 000 cm^{-1}). The first pure component spectrum is typical for Cr^{6+}, whereas the second pure component spectrum is indicative of the presence of $Cr^{2+/3+}$. Fig. 15 illustrates the effect of the reaction temperature and the support composition on the K–M($Cr^{2+/3+}$) (z) values. It is clear that the band intensity increases with increasing reaction temperature and IEP of the support.

In the final step, a mathematical relation which relates the dehydrogenation activity with the amount of in situ measured $Cr^{3+/2+}$ was derived. This is illustrated in Fig. 16 for Cr/Al_2O_3 catalysts. It can be concluded that the catalytic activity (response Y) is directly proportional to the amount of reduced Cr (response Z). The difference in catalytic activity between Cr/Al_2O_3 catalysts, which were 10 or 50 min on stream, must be explained in terms of coking. Finally, it is important to stress that the present analysis does not discriminate between Cr^{2+} and Cr^{3+}, and thus, does not allow to unambiguously assign the

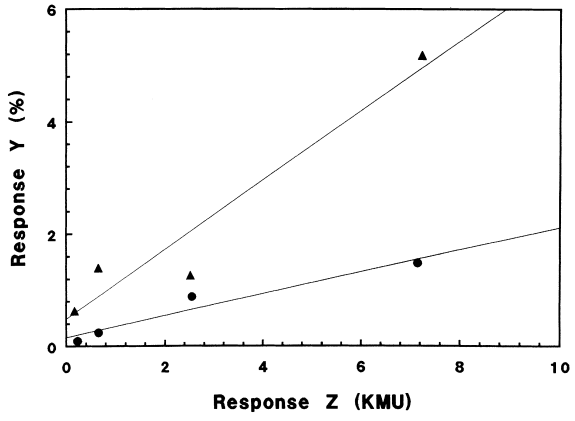

Fig. 16. Quantitative relationship between the catalytic activity (response Y) and the amount of reduced Cr (response Z) as predicted for (■) 10 and (●) 50 min on stream.

catalytic activity to one of these species. Thus, DRS spectroscopy alone is not sufficient to resolve this issue.

7. Reduction kinetics

The in situ DRS cell of Fig. 4 can also be used for the evaluation of the reduction kinetics of supported

metal oxide catalysts. This will be illustrated for the reduction of supported chromium oxide catalysts with CO [21].

The overall reduction reaction with CO can be represented as:

$$Cr_a + nCO \leftrightarrow Cr_r + nCO_2, \quad (7)$$

where Cr_a stands for anchored Cr^{6+}, and Cr_r for reduced Cr; i.e., mainly Cr^{3+} on alumina, and mainly Cr^{2+} on silica. The corresponding rate equation then is

$$\frac{d[Cr_a]}{dt} = k[Cr_a]^{\alpha}[CO]^{\beta} \quad (8)$$

which at constant partial pressure of CO becomes

$$\frac{d[Cr_a]}{dt} = k'[Cr_a]^{\alpha}. \quad (9)$$

Eq. (9) can be used to determine the kinetic parameters of the reduction if $[Cr_a]$ can be followed as a function of time at a constant temperature by quantitative DRS. The CT-band around 370 nm (27 000 cm^{-1}) of chromate/dichromate can be used for that purpose, if its intensity varies linearly with the amount of Cr. This is, as discussed above, the case for catalysts with small Cr content.

By measuring the $[Cr_a]$ versus time profiles as a function of the catalyst composition, reduction temperature and Cr loading, it was possible to derive a kinetic model, rate constants and reaction orders for the reduction process. The overall reaction order is between 2 and 3, which is exactly the same as was found by Finch [22] on the basis of a temperature programmed reduction study. Furthermore, the rate constants of the rate-determining step clearly indicate that reduction of Cr^{6+} on silica is faster than on alumina. A model to explain the kinetics is a two-step mechanism: the adsorption of CO to activate it and the reduction, which is rate-determining. On the basis of this model, we anticipate the presence of (i) adsorbed CO and (ii) surface carboxylates and carbonates on the surface, which were indeed observed by in situ FTIR measurements [23].

8. Concluding remarks and outlook

DRS in the UV–Vis–NIR region is a well-established spectroscopic technique which is based on known and easily accessible theories. This makes the interpretation of the DRS spectra relatively easy, whereas band decomposition routines and chemometrical techniques assist the user in a more detailed and quantitative analysis of the DRS spectra. It is clear that the DRS technique can be applied at different levels of sophistication: from merely detecting the presence of a certain oxidation state of a supported TMI up to a detailed distribution of different oxidation states and coordination environments under catalytic conditions.

However, the number of quantitative DRS studies is still very limited, and the authors hope that more quantitative studies on supported metal oxide catalysts will appear in the literature. Only by a systematic and intelligent application of the DRS technique, in conjunction with mathematical and statistical routines, can all the necessary information be extracted and fully appreciated. It is expected that such an approach will lead in the near future to a better understanding of the surface chemistry of supported metal oxide catalysts in catalytic action.

Acknowledgements

B.M.W. is a postdoctoral fellow of the Fonds voor Wetenschappelijk Onderzoek – Vlaanderen (FWO). This work was financially supported by the Geconcerteerde Onderzoeksactie (GOA) of the Flemish Government and by the FWO.

References

[1] G. Kortüm, Reflectance Spectroscopy, Springer, Berlin, 1969.
[2] R.A. Schoonheydt, in: F. Delannay (Ed.), Characterization of Catalysts, Marcel Dekker, 1984, p. 125.
[3] R. Kellerman, in: W.N. Delgass, G.L. Haller, R. Kellerman, J.H. Lunsford (Eds.), Spectroscopy in Heterogeneous Catalysis, Academic Press, New York, 1979, p. 86.
[4] K. Klier, in: A.T. Bell, M.L. Hair (Eds.), Vibrational Spectroscopies for Adsorbed Species, American Chemical Society Symposium Series, vol. 137, 1980, p. 141.
[5] R.A. Schoonheydt, in: J.J. Fripiat (Ed.), Advanced Methods in Clay Minerals Analysis, Elsevier, Amsterdam, 1981, p. 169.
[6] K. Klier, J. Opt. Soc. Am. 62 (1972) 882.
[7] B.M. Weckhuysen, I.E. Wachs, R.A. Schoonheydt, Chem. Rev. 96 (1996) 3327.
[8] Optical Spectroscopy: Sampling Techniques Manual, Harric Scientific, New York, 1987.
[9] B.M. Weckhuysen, L.M. De Ridder, R.A. Schoonheydt, J. Phys. Chem. 97 (1993) 4756.

[10] B.M. Weckhuysen, R.A. Schoonheydt, J.M. Jehng, I.E. Wachs, S.J. Cho, R. Ryoo, S. Kijlstra, E. Poels, J. Chem. Soc., Faraday Trans. 91 (1995) 3245.
[11] D.L. Massart, S.N. Vandeginste, Y. De Ming, Y. Michotte, L. Kaufmann, Chemometrics: A Textbook, Elsevier, Amsterdam, 1988.
[12] S. Wold, Chem. Int. Lab. Syst. 2 (1987) 37.
[13] P. Geladi, B.R. Kowalski, Anal. Chim. Acta 185 (1986) 1.
[14] M.J. Adams, Chemometrics in Analytical Spectroscopy, The Royal Society of Chemistry, Cambridge, 1995.
[15] W. Windig, J. Guilment, J. Anal. Chem. 63 (1991) 1425.
[16] W. Windig, C.E. Heckler, F.A. Agblevor, R. Evans, J. Chem. Int. Lab. Syst. 14 (1992) 195.
[17] W. Windig, D.A. Stephenson, Anal. Chem. 64 (1992) 2735.
[18] B.M. Weckhuysen, A.A. Verberckmoes, A.R. De Baets, R.A. Schoonheydt, J. Catal. 166 (1997) 160.
[19] B.M. Weckhuysen, A.A. Verberckmoes, J. Debaere, K. Ooms, I. Langhans, R.A. Schoonheydt, submitted.
[20] B.M. Weckhuysen, A. Bensalem, R.A. Schoonheydt, J. Chem. Soc., Faraday Trans. 94 (1998) 2011.
[21] A. Bensalem, B.M. Weckhuysen, R.A. Schoonheydt, J. Phys. Chem. B 101 (1997) 2824.
[22] J.N. Finch, J. Catal. 43 (1976) 111.
[23] A. Bensalem, B.M. Weckhuysen, R.A. Schoonheydt, J. Chem. Soc., Faraday Trans. 93 (1997) 4065.